3D Aeromagnetic Mapping of the Williston Basin Basement*

Jiakang Li[1] and Igor Morozov[1]

[1]University of Saskatchewan, Saskatoon, Saskatchewan, Canada (jiakang.li@usask.ca)

Abstract

Regional magnetic anomalies are sensitive to the variations of the structure and composition of the crystalline basement. Most bodies within the basement have distinctive magnetic signatures which are characterized by their magnitudes, heterogeneity, and magnetic fabric. When calibrated with known geology, basement structures can often be mapped from aeromagnetic data under the cover of sedimentary rock.

The most important and accurate information provided by magnetic data is the structural fabric of the basement. Major basement structures can be interpreted from consistent discontinuities and/or pattern breaks in the magnetic fabric. Once the structures have been evaluated, correlated, and combined with those interpreted from the gravity data, a model for the evolution of the basement and overlying basins can be developed.

In this study, we focus on direct magnetic basement depth estimation from grid aeromagnetic data within the Saskatchewan and Manitoba parts of the Williston Basin. The objective is to produce a seamless and integrated interpretation of the basement and extend the previous interpretations by Miles et al. (1997), Kreis et al. (2000), and Pilkington and Thomas (2001). We analyse patterns observed in several attribute maps derived from aeromagnetic grids, invert for basement depth, and identify domain boundaries and structural patterns. The magnetic source inversion technique is employed and calibrated using well log data. The resulting depth maps are interpreted for structural fabric, revealing several groups of linear magnetic contrasts at different scale lengths.

Data

The study region includes 15,737,915 aeromagnetic survey values interpolated on a 200-m grid covering southeastern Saskatchewan and southwestern Manitoba (Figure 1). In addition to this data, information from 239 logs from boreholes penetrating the Precambrian basement was used to constrain the basement depth estimation.

Processing and Inversion

Prior to the inversion, the data required preparation and pre-processing. The key processing steps included:

1) Reduction to the pole, which reduces the effect of the Earth's ambient magnetic field and provides a more accurate determination of the position of source bodies. A constant direction of the background magnetic field with declination of 9º and inclination of 75º was used for the area.

2) First and second derivatives, which are commonly used to delineate the boundaries of source bodies and local anomalies.

3) Downward continuation reducing the survey surface to 1 km above the basement. This procedure removes the effects of elevation of the basement and improves resolution (Pilkington and Roest, 1992; Li and Morozov, 2004).

Two methods for basement depth estimation were employed, yielding comparable yet complementary results. The first method was based in Euler deconvolution, and the second utilized the spatial-domain local wavenumber attributes.

1) Euler Deconvolution Method

In the case of grid data, the Euler equation becomes (Thompson, 1982; and Reid et al., 1990):

$$(x - x_0)\frac{\partial}{\partial x}P(x,y,z) + (y - y_0)\frac{\partial}{\partial y}P(x,y,z) + (z - z_0)\frac{\partial}{\partial z}P(x,y,z) = (B - \eta)\cdot P(x,y,z)$$

Here (x_0, y_0, z_0) is the position of the top of the source, (x, y, z) is the location of the field measurement, P is the field intensity anomaly value, B is the background field, and η is the Euler structural index.

The method operates by solving the above over-determined equation using the least-squares method within a sliding square data window, and results in the source coordinates (x_0, y_0, z_0). In this study, by testing after several trial values and comparing the results to the basement model based on well log data, the structural index η was chosen to be 0.45, and the window size was kept variable and proportional to the average depth of the basement. SVD was employed to solve a series of (moving window size) ×4 least-squares equations. The resulting source coordinates (x_0, y_0, z_0) were finally interpolated to form a map of source distributions within the study area.

2) Local-Wavenumber Method

The depth of the Precambrian basement was also inverted by using the local wavenumber technique (Thurston and Smith, 1997). Similar to Euler Deconvolution, this method allows us to obtain an estimate of the depth that with only limited assumptions about the model. For a specific shape and position of the source, its local depth can be directly estimated by inverting the local wavenumber.

The local wavenumber attributes were extracted by using the Tilt derivative approach (Fairhead, 2004; Smith, 1998; Thurston, 1997; Verduzco, 2004; Li and Morozov, 2005). Using the following attributes:

Tilt derivative (TDR):

$$TDR = \tan^{-1}(T_z / \sqrt{T_x^2 + T_y^2})$$

Total horizontal derivative of TDR:

$$TDR\_THDR = \sqrt{\left(\frac{\partial TDR}{\partial x}\right)^2 + \left(\frac{\partial TDR}{\partial y}\right)^2}.$$

These operations suppress the longer-wavelength anomalies and emphasize the effects of the sedimentary cover and of the basement. Because it is based on the second and higher derivatives, the Local-Wavenumber technique provides high-resolution image, in which the subdomain structures and boundaries and magnetic lineations are displayed in more detail (Figure 2).

Interpretation

The structural pattern of the basement as revealed from combined gravity and magnetic interpretations can be characterized by a hierarchy of structural elements. We distinguish three tiers in this classification: (1) large structural zones, (2) tectonic domains, and (3) sub-domains and internal magnetic lineaments. On top of this structure, there also appear additional extended features that overprint some of these structures and are potentially related to deposition of basin sediments.

The main boundaries that delineate units of the first structural class within the basin can be identified from correlating the aeromagnetic and gravity maps and their horizontal and vertical derivatives. These first structural zones are quite apparent from the changes in the amplitude and gradient patterns, and also from surface geology (e.g. Kreis et al., 2000), and represent (east to west) the Superior Province, Churchill-Superior Boundary Zone, Reindeer Zone, Sask-Reindeer Boundary Zone, Sask Craton, and Wyoming Craton.

In our interpretation, major basement blocks and structural contrasts are identified from the horizontal and vertical gradients and attribute maps. Domain boundaries are then delineated by the areas of parallel or perpendicular trends that have comparable amplitudes of the anomalies. After these structures were identified, we may extract the smaller-scale possible lineaments based on the local-wavenumber magnetic attributes (Figure 2). The Precambrian basement depth map (Figure 3) based on Euler method expresses the outline of basement topography with depth region from 300 m to -4000 m, the shallow parts are in the edge of Shield and the deepest is at the south of Weyburn. The depth map plus interpreted boundaries of domains based on magnetic data reveals the complex block structure pattern of the Williston Basin. Similar structures may also exist in the deeper parts of the basin, as indicated by identification of major basement faults in several seismic studies (Hajnal et al., 1996).

Conclusions

Combining the horizontal and total gradient, local wavenumber attributes and Euler deconvolution depth estimation mapping offers an improved horizontal resolution to the conventional methods and a way of estimating depths to the basement topography. These methods contribute to the geophysical information about structural pattern and domain definition of the Williston Basin.

Acknowledgements

References Cited

Fairhead, J.D., S.E. William, and G. Flanagan, 2004, Testing magnetic local wavenumber depth estimation methods using a complex 3D model: Society of Exploration Geophysicists, 2004 Expanded Abstracts, p. 742-745.

Hajnal, Z., S. Lucas, D. White, J. Lewry, S. Bezdan, M.R. Stauffer, and M.D. Thomas, 1996, Seismic reflection images of high-angle faults and linked detachments in the Trans-Hudson Orogen: Tectonics, v. 15, p. 427-439.

Kreis, L.K., K.E. Ashton, and R.O. Maxeiner, 2000, Interpretive geophysical maps of Saskatchewan: Saskatchewan Energy Mines, Open File Report 2000-2.

Li, J., and I. Morozov, 2004, Continuous equivalent source surface approach for accurate interpolation and continuation: 2004 CSEG, Calgary.

Li, J., and I. Morozov, 2005, Potential field investigation of Williston Basin basement: 2005 CSEG, Calgary.

Miles, W., P.E. Stone, and M.D. Thomas, 1997, Magnetic and gravity maps with interpreted Precambrian basement, Saskatchewan, Scale 1:1,500,000, GSC Open file 3488.

Reid, A.B., J.M. Allsop, H. Granser, A.J. Millete, and I.W. Somerton, 1990, Magnetic interpretation in three dimensions using Euler deconvolution: Geophysics, v. 55, p. 80-91.

Pilkington, M., and W.R. Roest, 1992, Draping aeromagnetic data in areas of rugged topography: J. Appl. Geophys., v. 29, p. 135-142.

Pilkington, M., and M.D. Thomas, 2001, Magnetic and gravity maps with interpreted Precambrian basement, Manitoba, Scale 1:1,500,000, GSC Open file 3739.

Smith, R.S., J.B. Thurston, T.F. Dai, and I.N. MacLeod, 1998, iSPI™ - the improved source parameter imaging method: Geophysical Prospecting, v. 46, p. 141-151.

Thompson, D.T., 1982, EULDPH: A new technique for making computer-assisted depth estimates from magnetic data: Geophysics, v. 47, p. 31-37.

Thurston, J.B., and R.S. Smith, 1997, Automatic conversion of magnetic data to depth, dip, and susceptibility contrast using the SPI™ method: Geophysics, v. 62, p. 807-813.

Verduzco, B., J.D. Fairhead, and C. MacKenzie, 2004, New insights into magnetic derivatives for structural mapping: The Leading Edge, v. 24, p. 116-119.
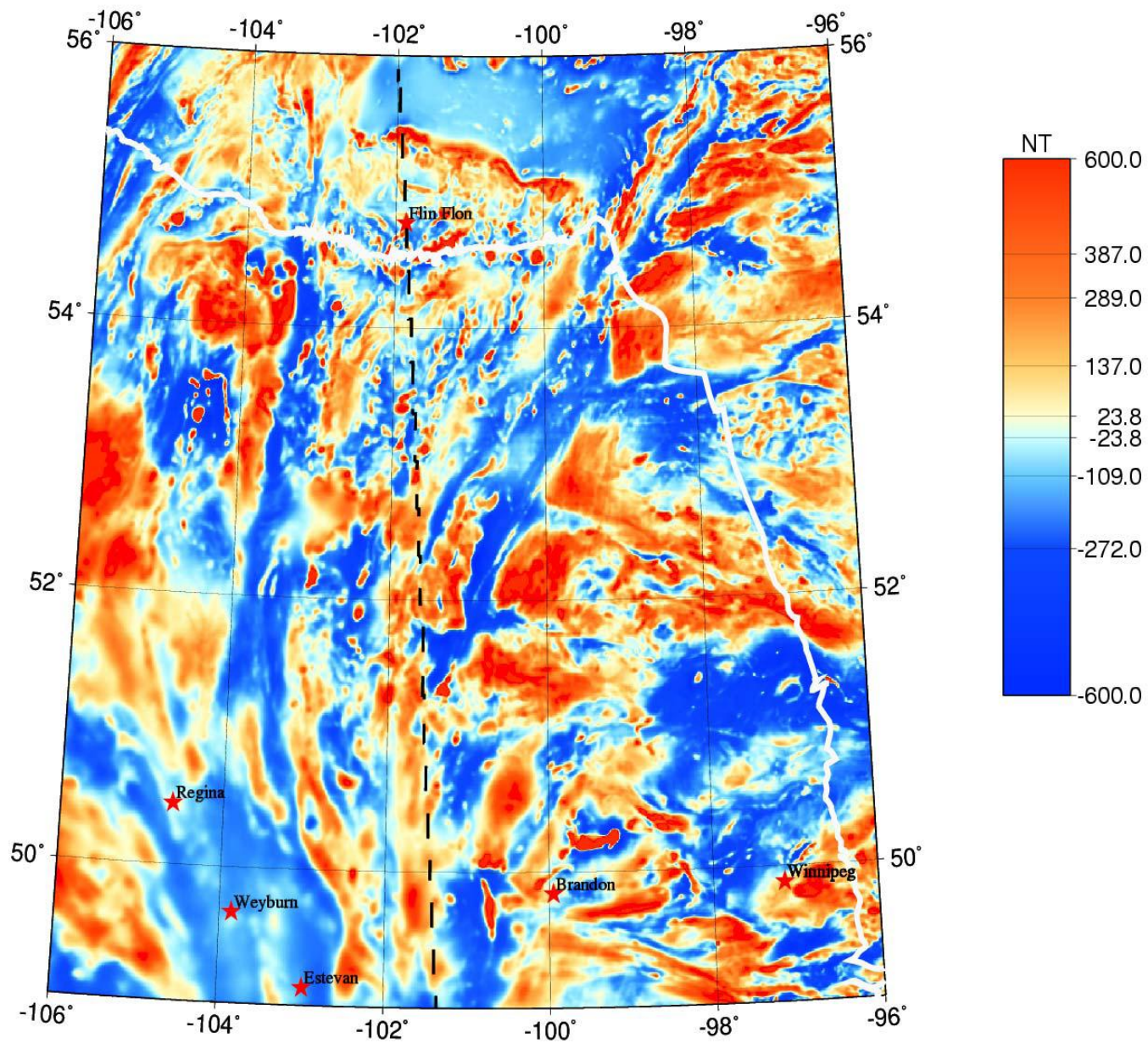
Figure 1. Map of aeromagnetic anomaly interpolated and reduced to the pole. White line indicates the edge of the Canadian Shield.
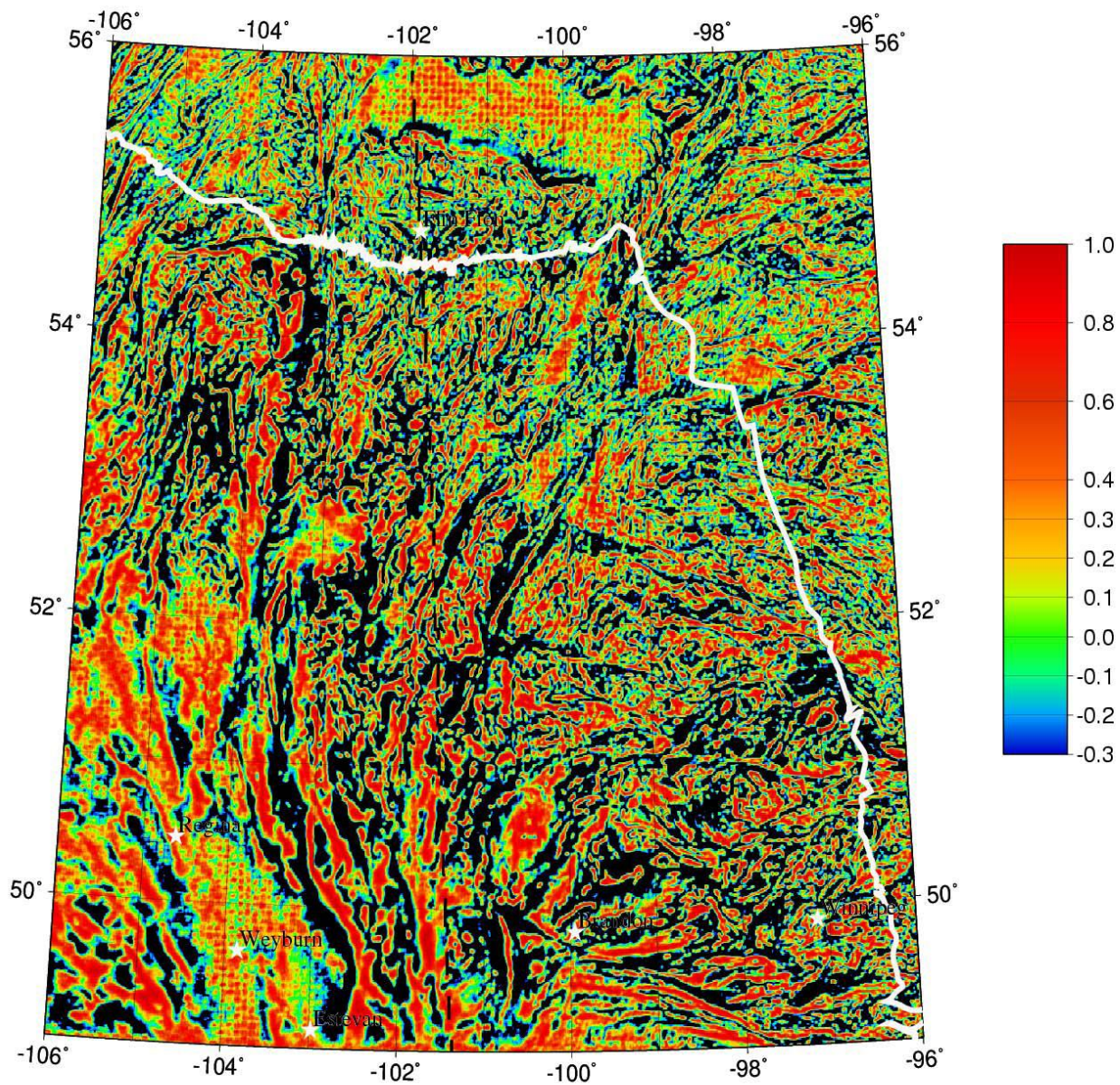
Figure 2. Local Wavenumber image providing high-resolution delineation of magnetic source anomalies. These features are very useful to the analysis of local and regional structure of basin.
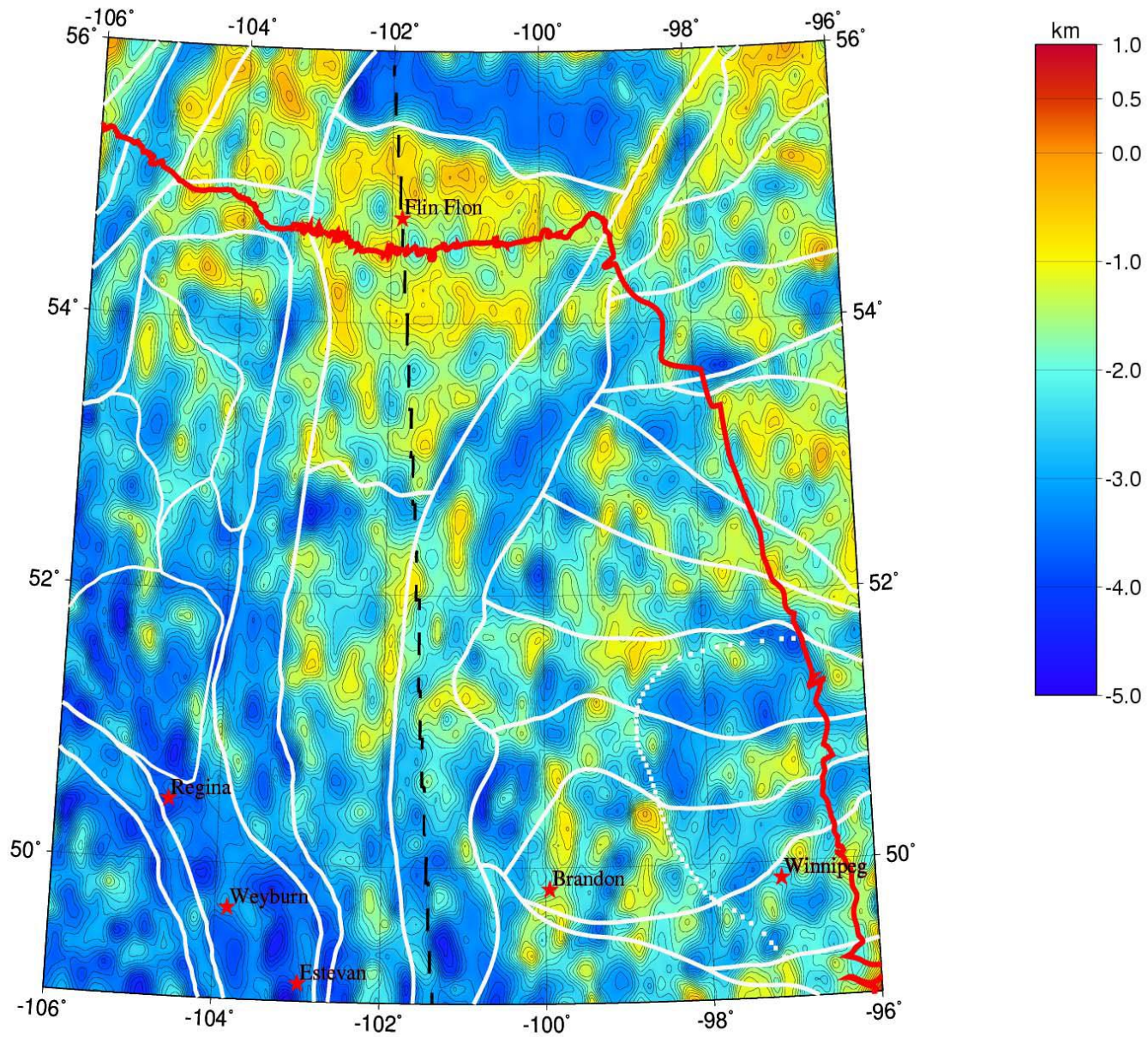
Figure 3. Euler Deconvolution result, including constraints from logs and seismic data. The red line is the edge of the Canadian Shield. White lines are the interpreted domain boundaries.